Structural and Dielectric Properties of Manganese Ferrite Nanoparticles

Hashim Farooq[1], Muhammad Raza Ahmad[1], Yasir Jamil[1,*], Abdul Hafeez[2], Zeeshan Mahmood[1] and Tahir Mahmood[1]

[1]*Department of Physics, University of Agriculture, Faisalabad, Pakistan*

[2]*Government Elementary Teachers Training College, Samanabad, Faisalabad, Pakistan*

Abstract: In this work, Manganese ferrite nanoparticles of various compositions were reproducibly synthesized *via* coprecipitation route. Variation in structural and dielectric properties was studied by varying the sintering temperature, sintering time and manganese to iron ratio. Structural, compositional and phase properties were investigated by X-ray diffraction (XRD) technique which confirmed the pure normal spinel structure with no other phase/impurity. Particle size, Lattice constant, measured bulk density, X-ray density, Specific Surface Area and Porosity were determined by the standard formulae. Responses of Capacitance and Dielectric constant were studied at room temperature in the frequency range of 600Hz to 1MHz by LCR meter which both showed the exponential decay at low frequency while both became nearly independent of frequency in higher frequency ranges.

Keywords: Nanoparticles, spinel structure, coprecipitation, dielectric constant.

1. INTRODUCTION

Nano particles exhibit different properties compared to the corresponding bulk materials [1, 2]. Important characteristics of ferrites are their high values of resistivity and low eddy current losses which make them ideal for high frequency applications [3]. The recent technological advances in electronics need more compact cores for work at higher frequencies [1]. Manganese ferrites ($MnFe_2O_4$) belong to a technologically important group of transition metal ferrites with many well known specialized applications [4, 5]. Manganese ferrites exhibit magnetization of different orders of magnitude even if having the similar size of particles due to the inversion of Mn and Fe ions over sites [6-9].

Spinel ferrite nanoparticles have great importance in nanoscience and nanotechnology for technological applications because of their outstanding properties such as nanometer size and large surface area to volume ratio [6, 10, 11]. $MnFe_2O_4$ is an important member of spinel structured ferrite family [10]. $MnFe_2O_4$ have potential applications in electronic [4, 12] and telecommunication [12] industries like dry cell batteries [13], thermochemical water-splitting process [14], inductance components [15], microwave devices [3, 8, 15], high density magnetic recording [1-4, 8, 12, 15], switching devices [3,15], phase shifter and other high frequency devices [2, 3, 8], sensor technology [8], ferro fluids [1-3, 12], catalyst [12], photocatalytic [9], magnetic refrigerators [2] and biomedical applications [9,15] like targeted drug delivery [1, 3, 9, 15, 16] and MRI contrast agents [17].

The synthesis of nanocrystalline spinel manganese ferrite has been investigated extensively in recent years due to their structural, thermal, physical [3, 12], chemical and particularly due to their magnetic properties [6, 9, 10]. Moreover, the synthesis route also plays a pivotal role because samples of comparable crystallite size prepared by different processes show different magnetic properties. In recent years, $MnFe_2O_4$ NPs prepared using varied methods, such as solid state reaction method [3, 8, 15, 18], sol-gel technique [14], hydrothermal/solvothermal method [9], chemical coprecipitation technique [1, 2, 10, 11, 19-23], citrate precursor technique [12], combustion technique [5, 6], freeze-drying route [4], reverse micelle technique [24] have been extensively studied. Aggregation and coarsening of particles at elevated temperatures is a critical obstacle in majority of the above mentioned synthesis techniques [24]. Of all these techniques, chemical coprecipitation route seems to be the most convenient for the synthesis of NPs because of its simplicity, cost effectiveness, less time consuming, high mass production and better control over crystallite size, homogeneity, morphology and other properties of the materials in addition to low cost [1, 11, 21-29]. Current research efforts are being directed to synthesize Size-controllable $MnFe_2O_4$ nanoparticles by coprecipitation route and to make detailed study of structural and dielectric properties by varying sintering conditions.

*Address corresponding to this author at the Department of Physics, University of Agriculture, Faisalabad, Pakistan; Tel: 041-9200109;
E-mail: yasirjamil@yahoo.com

ISSN: 1814-8085 / E-ISSN: 1927-5129/12

Experimental Procedure

The structural and dielectric properties of manganese ferrites depend upon on the manganese to iron Mn:Fe mole ratio, sintering conditions and temperature treatment [18]. In this study, chemical coprecipitation route was adopted to synthesize Mn-ferrite NPs. The metal ion solution was prepared by adding chlorides of manganese and ferric into distilled and deionized water. A 1-molar solution of NaOH was prepared separately in doubly distilled, deionized water. The solution containing the metal ions was mixed drop wise into the NaOH solution with rigorous mechanical stirring on a magnetic stirrer. The solution thus formed kept under isothermal static conditions in a preheated water bath four hours. The precipitates were filtered and washed with deionized water till a pH=7 was obtained and then dried in an oven at 60^{o}C. The powders were pressed into pellets form at 8,000 psi pressure.

Manganese ferrite NPs were characterized for structural and compositional properties at room temperature using PANalytical X-ray diffractometer system with CuKα (λ=1.5406Å) at a scanning rate of 1^{o} min^{-1} in 2θ range of 2 to 80 degree. For the measurement of dielectric constant of the samples, silver paint was applied on the flat surfaces of the pellets and air-dried to have good ohmic contacts. The capacitance of the samples was measured using a WAYNE KERR 4275 LCR Meter Bridge at room temperature and then the dielectric constant was calculated with changing frequency in the range of 60Hz to 1MHz.

2. RESULTS

The structure and crystallite size of prepared manganese ferrite samples were determined by XRD analysis. All the observed peaks correspond to standard spinel diffraction patterns with no extra peak which confirmed the single phase cubic structure. The XRD pattern showed that the strongest reflection come from the (311) plane for all the samples. The Particle size, measured bulk density and X-ray density were calculated by the equations (1), (2) and (3) respectively.

$$D_{(311)} = 0.89\lambda / \beta \cos\theta \quad (1)$$

$$\rho_m = m / \pi r^2 h \quad (2)$$

$$\rho_x = 8M / Na^3 \quad (3)$$

Equation (1) represents the Debye-Sherrer's formula, in which $D_{(311)}$ is the crystallite size calculated from the most intense peak having miller indices (3 1 1), λ is the wavelength of CuKα (0.15406nm), θ is the corresponding diffraction angle, 0.89 is the Sherrer's constant and B is the full width at half maximum of the peak in radian [8]. Strong peaks are only expected when the Bragg condition is satisfied [30]. In equation (2), *m* is the mass, *r* is the radius and *h* is the thickness of pellet. In equation (3), *M* is the molecular weight of the samples, *N* is the Avogadro's number and '*a'* is the lattice parameter. Moreover, Specific Surface Area and Porosity were determined by the equation numbers (4) and (5) respectively.

$$S = 6000 / \rho_x D \quad (4)$$

$$P = 1 - \left(\rho_m / \rho_x \right) \quad (5)$$

In equation (4), D is the crystallite size and ρ_x is the x-ray density. In equation (5), ρ_m is the measured bulk density and ρ_x is the x-ray density.

The effect of frequency on the dielectric constant has been studied for all the samples. The dielectric constant of all the samples have measured in the frequency range of 60Hz to 1MHz by equation (6). In this equation, C is the capacitance of the pellet, d is the

Table 1: Showing the Particle Size, Lattice Constant, X-Rays Density, Measured Bulk Density, Porosity, Specific Surface Area

Sr. No	Sample Code	Mn:Fe Ratio	Temp, ^{o}C	Time, hr	Particle size, nm	Lattice constant, A	Measured Bulk Density, g/cm^3	X-ray density, g/cm^3	% Porosity	Specific Surface Area, cm^2/g
	6B	0.2	800	8	85	8.4	2.102	5.1628142	59.286	1.000000x10^8
	3B	0.2	800	4	60	8.35	2.2	5.2629771	58.199	1.9000653x10^8
	6A	0.1	800	8	15	8.37	2.02615	5.2816076	61.638	1.757301 x10^8
	3A	0.1	800	4	70	8.39	2.026	5.1880323	60.949	1.652154x10^7

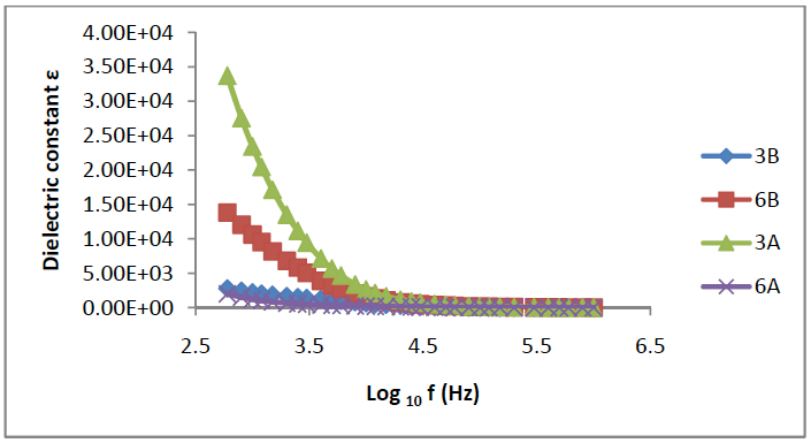

Figure 1: Variation in Dielectric constant (ε′) with increasing frequency for 3B, 6B, 3A and 6A.

thickness of the pellet, A is the Cross-sectional area of the flat surface of the pellet and ε_o is the permittivity constant of free space.

$$\varepsilon' = Cd/A\varepsilon_o \quad (6)$$

3. DISCUSSION

Many research groups are taking keen interest to study the structural and dielectric properties of nanocrystalline spinels [24]. Spinel structure is made up of a close-packed fcc array of oxygen atoms in which tetrahedral and octahedral interstitial sites are occupied by cations. XRD patterns showed the pure single phase structure [2]. The lattice constant does not show any significant change with increasing particle size [2]. Various properties of ferrites are greatly influenced by the distribution of cations among the sublattices, nature of crystal (shape, size and orientation), crystal boundaries, surface layers and contacts etc [3].

In the samples 6B and 3B, Mn:Fe ratio was kept 0.2. 6B was treated at 800C for 8 hours and 3B was treated at the same temperature for 4 hours. In the samples 6A and 3A, Mn:Fe ratio was kept 0.1 and both were treated at 800C but 6A was treated for 8 hours and 3A was treated for 4 hours. Variation in structural parameters due to changing sintering time has listed in the Table **1**.

The effect of frequency on the dielectric constant has been studied. Dielectric constant was measured in the range of 600Hz to 1MHz which exponentially decreased with increasing frequency and this variation in dielectric constant is due to the space charge polarization. In the frequency range, the dielectric constant initially decreased with frequency then reached a constant value at higher frequency range as shown in the Figure **1**. The value of dielectric constant is much higher at lower frequencies. It decreases with the increase in frequency in lower frequency while at very high frequencies its value becomes so small that it becomes independent of frequency. The variation in dielectric constant may be explained on the basis of space–charge polarization produced due to the presence of higher conductivity phases in the grain boundaries of a dielectric, which produces localized accumulation of charge under the influence of an electric field. The assembly of space charge carriers in a dielectric takes a finite time to line up their axes parallel to an alternating electric field. If the frequency of the field reversal increases, a point is reached where the space charge carriers cannot keep up with the field and, the alternation of their direction lags behind that of the field. This results in a reduction in the dielectric constant of the material. According to Maxwell and Wagner two-layer model, space–charge polarization is because of the inhomogeneous dielectric structure of the material. It was observed that in the low frequency range, the rate of exponential decay of dielectric constant in 3A and 6B is faster than that of 3B and 6A. Very little work is done to the best of my knowledge on the dielectric behavior of Mn ferrites however same exponential trend is found for other mixed ferrites as discussed by [3, 25-40].

4. CONCLUSIONS

The synthesis of $MnFe_2O_4$ powders through coprecipitation technique resulted in the formation of highly crystalline $MnFe_2O_4$ spinel particles, homogeneously distributed with small particle size. Single phased nanosize manganese ferrites were successfully synthesized through a simple and versatile

synthetic procedure. The characterization results showed the small nanoparticle size and large surface area. The synthesized NPs exhibit the pure cubic spinel phase. The dispersion in dielectric properties have been explained in the light of Maxwell–Wagner model. Sintering temperature, sintering time and Manganese to iron ratio affects most of the structural and dielectric properties of Mn ferrites.

ACKNOWLEDGEMENTS

Pakistan Science Foundation (PSF), Pakistan is highly acknowledged for funding this research work under grant number PSF/Res/P-AU/Phys(151).

REFERENCES

[1] Musat V, Potecasu O, Belea R, Alexandru P. Magnetic materials from co-precipitated ferrite nanoparticles. Mater Sci Eng B 2010; 167: 85-90. http://dx.doi.org/10.1016/j.mseb.2010.01.038

[2] Raghavender AT, Hong NH. Dependence of Neel temperature on the particle size of $MnFe_2O_4$. J Magnet Magnet Mater 2011; 323: 2145-47. http://dx.doi.org/10.1016/j.jmmm.2011.03.018

[3] Batoo KM. Study of dielectric and impedance properties of Mn ferrites. Physica B 2011; 406: 382-87. http://dx.doi.org/10.1016/j.physb.2010.10.075

[4] Bellini JV, de Medeiros SN, Ponzoni ALL, Longen FR, de Melo MAC, Paesano A Jr. Manganese ferrite synthesized from Mn(II) acetate + hematite freeze-dried powders. Mater Chem Phys 2007; 105: 92-98. http://dx.doi.org/10.1016/j.matchemphys.2007.04.005

[5] Deraz NM, Shaban S. Optimization of catalytic, surface and magnetic properties of nanocrystalline manganese ferrite. J Anal Appl Pyrolysis 2009; 86: 173-79. http://dx.doi.org/10.1016/j.jaap.2009.05.005

[6] Li Y, Jiang J, Zhao J. X-ray diffraction and Mössbauer studies of phase transformation in manganese ferrite prepared by combustion synthesis method. Mater Chem Phys 2004; 87: 91-95. http://dx.doi.org/10.1016/j.matchemphys.2004.05.007

[7] Chlan V, Prochazka V, Stepankova H, Sedlak B, Novak P, Simsa Z, Brabers VAM. ^{57}Fe NMR study of manganese ferrites. J Magnet Magnet Mater 2008; 320: e96-e99. http://dx.doi.org/10.1016/j.jmmm.2008.02.022

[8] Lazarevic ZZ, Jovalekic C, Recnik A, *et al*. Study of manganese ferrite powders prepared by a soft mechanochemical route. J Alloys Comp 2011; 509: 9977-85. http://dx.doi.org/10.1016/j.jallcom.2011.08.004

[9] Guo P, Zhang G, Yu J, Li H, Zhao XS. Controlled synthesis, magnetic and photocatalytic properties of hollow spheres and colloidal nanocrystal clusters of manganese ferrite. Colloids and Surfaces A: Physicochem Eng Aspects 2012; 395: 168-74. http://dx.doi.org/10.1016/j.colsurfa.2011.12.027

[10] Siddique M, Butt NM. Effect of particle size on degree of inversion in ferrites investigated by Moossbauer spectroscopy. Physica B 2010; 405: 4211-15.s http://dx.doi.org/10.1016/j.physb.2010.07.012

[11] Pereira C, Pereira AM, Fernandes C, *et al*. Superparamagnetic MFe_2O_4 (M = Fe, Co, Mn) Nanoparticles: Tuning the Particle Size and Magnetic Properties through a Novel One-Step Coprecipitation Route. Chem Mater 2012; 24: 1496-504.

[12] Ahmed MA, El-dek SI, Mansour SF, Okasha N. Modification of Mn nanoferrite physical properties by gamma, neutron, and laser irradiations. Solid State Sci 2011; 13: 1180-86. http://dx.doi.org/10.1016/j.solidstatesciences.2010.10.027

[13] Belardi G, Lavecchia R, Medici F, Piga L. Thermal treatment for recovery of manganese and zinc from zinc-carbon and alkaline spent batteries. Waste Management 2012. http://dx.doi.org/10.1016/j.wasman.2012.05.008

[14] Bhosale RR, Shende RV, Puszynski JA. Thermochemical water-splitting for H2 generation using sol-gel derived Mn-ferrite in a packed bed reactor. Int J Hydrogen Energy 2012; 37: 2924-34. http://dx.doi.org/10.1016/j.ijhydene.2011.03.010

[15] Chen D, Liu HY, Li L. One-step synthesis of manganese ferrite nanoparticles by ultrasonic wave-assisted ball milling technology. Mater Chem Phys 2012; 134: 921e924. http://dx.doi.org/10.1016/j.matchemphys.2012.03.091

[16] Francolini I, Palombo M, Casini G, *et al*. Novel manganese-ferrite nanocomposites for targeted delivery of anticancer drugs. J Control Release 2010; 148: e57-e73. http://dx.doi.org/10.1016/j.jconrel.2010.07.021

[17] Yang H, Zhang C, Shi X, *et al*. Water-soluble superparamagnetic manganese ferrite nanoparticles for magnetic resonance imaging. Biomaterials 2010; 31: 3667-73. http://dx.doi.org/10.1016/j.biomaterials.2010.01.055

[18] Ahmed YMZ. Synthesis of manganese ferrite from non-standard raw materials using ceramic technique. Ceramics Int 2010; 36: 969-77. http://dx.doi.org/10.1016/j.ceramint.2009.11.020

[19] Mozaffari M, Behdadfar B, Amighian J. Preparation and Characterization of Manganese Ferrite Nanoparticles *via* Co-precipitation Method for Hyperthermia. Iranian J Pharm Sci 2008; 4(2): 115-18.

[20] Elahi I, Zahira R, Mehmood K, Jamil A, Amin N. Co-precipitation synthesis, physical and magnetic properties of manganese ferrite powder. Afr J Pure Appl Chem 2012; 6(1): 1-5.

[21] Jamil Y, Ahmad MR, Hafeez A, Zia-ul-Haq, Amin N. Microwave Assisted Synthesis Of Fine Magnetic Manganese Ferrite Particles Using Co-Precipitation Technique. Pak J Agri Sci 2008; 45(3).

[22] Rashad MM. Synthesis and magnetic properties of manganese ferrite from low grade manganese ore. Mater Sci Eng B 2006; 127: 123-29. http://dx.doi.org/10.1016/j.mseb.2005.10.004

[23] Burojeanu VM, Fournés L, Wattiaux A, Etourneau J, Segal E. Cations distribution and magnetic properties of manganese ferrite powder prepared by coprecipitation from MnO and FeSO ?7H O 2 4 2. Int J Inorg Mater 2001; 3: 525-29.

[24] Misra RDK, Gubbala S, Kale A, Egelhoff WF, Jr. A comparison of the magnetic characteristics of nanocrystalline nickel, zinc, and manganese ferrites synthesized by reverse micelle technique. Mater Sci Eng B 2004; 111: 164-74. http://dx.doi.org/10.1016/j.mseb.2004.04.014

[25] Maqsood A, Khan K. Structural and microwave absorption properties of $Ni_{(1-x)}Co_{(x)}Fe_2O_4$ ($0.0 \leq x \leq 0.5$) nanoferrites synthesized *via* co-precipitation route. J Alloys Comp 2011; 509: 3393-97. http://dx.doi.org/10.1016/j.jallcom.2010.12.082

[26] Naeem M, Shah NA, Gul IH, Maqsood A. Structural, electrical and magnetic characterization of Ni-Mg spinel ferrites. J Alloys Comp 2009; 487: 739-43. http://dx.doi.org/10.1016/j.jallcom.2009.08.057

[27] Ashiq MN, Iqbal MJ, Gul IH. Structural, magnetic and dielectric properties of Zr-Cd substituted strontium hexaferrite ($SrFe_{12}O_{19}$) nanoparticles. J Alloys Comp 2009; 487: 341-45. http://dx.doi.org/10.1016/j.jallcom.2009.07.140

[28] Gul IH, Amin F, Abbasi AZ, Anis-ur-Rehman M, Maqsood A. Physical and magnetic characterization of co-precipitated nanosize Co-Ni ferrites. Scripta Mater 2007; 56: 497-500. http://dx.doi.org/10.1016/j.scriptamat.2006.11.020

[29] Gul IH, Maqsood A, Naeem M, Ashiq MN. Optical, magnetic and electrical investigation of cobalt ferrite nanoparticles synthesized by co-precipitation route. J Alloys Comp 2010; 507: 201-206. http://dx.doi.org/10.1016/j.jallcom.2010.07.155

[30] Hosseini SH, Mohseni SH, Asadnia A, Kerdarid H. Synthesis and microwave absorbing properties of polyaniline/MnFe2O4 nanocomposite. J Alloys Comp 2011; 509: 4682-87. http://dx.doi.org/10.1016/j.jallcom.2010.11.198

[31] Ajmal M, Maqsood A. Structural, electrical and magnetic properties of $Cu_{1-x}Zn_xFe_2O_4$ ferrites ($0 \leq x \leq 1$). J Alloys Comp 2008; 460: 54-59. http://dx.doi.org/10.1016/j.jallcom.2007.06.019

[32] Ajmal M, Shah NA, Maqsood A, Awan MS, Arif M. Influence of sintering time on the structural, electrical and magnetic properties of polycrystalline $Cu_{0.6}Zn_{0.4}Fe_2O_4$ ferrites. J Alloys Comp 2010; 508: 226-32. http://dx.doi.org/10.1016/j.jallcom.2010.08.067

[33] Ajmal M, Maqsood A. Influence of zinc substitution on structural and electrical properties of $Ni_{1-x}Zn_xFe_2O_4$ ferrites. Mater Sci Eng B 2007; 139: 164-70. http://dx.doi.org/10.1016/j.mseb.2007.02.004

[34] Ashiq MN, Iqbal MJ, Gul IH. Effect of Al-Cr doping on the structural, magnetic and dielectric properties of strontium hexaferrite nanomaterials. J Magnet Magnet Mater 2011; 323: 259-63. http://dx.doi.org/10.1016/j.jmmm.2010.08.054

[35] Atif M, Nadeem M, Grossinger R, Turtelli RS. Studies on the magnetic, magnetostrictive and electrical properties of sol-gel synthesized Zn doped nickel ferrite. J Alloys Comp 2011; 509: 5720-24. http://dx.doi.org/10.1016/j.jallcom.2011.02.163

[36] Atta-ur-Rahman, Rafiq MA, Karim S, Maaz K, Siddique M, Hasan MM. Reduced conductivity and enhancement of Debye orientational polarization in lanthanum doped cobalt ferrite nanoparticles. Physica B 2011; 406: 4393-99. http://dx.doi.org/10.1016/j.physb.2011.08.094

[37] Gul IH, Maqsood A. Structural, magnetic and electrical properties of cobalt ferrites prepared by the sol-gel route. J Alloys Comp 2008; 465: 227-31. http://dx.doi.org/10.1016/j.jallcom.2007.11.006

[38] Gul IH, Pervaiz E. Comparative study of $NiFe_{2-x}Al_xO_4$ ferrite nanoparticles synthesized by chemical co-precipitation and sol-gel combustion techniques. Mater Res Bull 2012; 47: 1353-61. http://dx.doi.org/10.1016/j.materresbull.2012.03.005

[39] Hussain S, Maqsood A. Influence of sintering time on structural, magnetic and electrical properties of Si-Ca added Sr-hexa ferrites. J Magnet Magnet Mater 2007; 316: 73-80. http://dx.doi.org/10.1016/j.jmmm.2007.03.206

[40] Iqbal MJ, Ashiq MN, Gul IH. Physical, electrical and dielectric properties of Ca-substituted strontium hexaferrite ($SrFe_{12}O_{19}$) nanoparticles synthesized by co-precipitation method. J Magnet Magnet Mater 2010; 322: 1720-26. http://dx.doi.org/10.1016/j.jmmm.2009.12.013

Received on 12-09-2012 Accepted on 09-10-2012 Published on 16-10-2012

http://dx.doi.org/10.6000/1927-5129.2012.08.02.53